Intelligent Characterisation of Satellites from Hyperspectral Time Series Analysis

Lewis Walker[1], Massimiliano Vasile[1], Andrew Campbell[2], Paul Murray[2], Stephen Marshall[2], and Vasili Savitski[3]

[1] Department of Mechanical and Aerospace Engineering, University of Strathclyde, 75 Montrose St, Glasgow, UK, G1 1XQ
[2] Department of Electronic and Electrical Engineering, 75 Montrose St, University of Strathclyde, Glasgow, UK, G1 1XQ
[3] Fraunhofer UK Centre for Applied Photonics, Technology and Innovation Centre, 99 George St, G1 1RD

Keywords: Machine learning · Hyperspectral imaging · Satellite characterisation

1 Introduction

Spectroscopy and spectral analysis have been shown in many previous studies to be useful for characterising and distinguishing satellites and space objects based on their spectral signatures [1–7], which are themselves characterised by the constituent materials as well as the lighting conditions. Previous work, however, has been mainly geared towards differentiating objects based purely on the spectrum [1, 5], or inferring the presence of certain materials from characteristic spectral peaks and troughs [1]. Previous works have generally considered only presence, and not abundance, of individual materials. Time-varying spectral signatures due to object rotation have been investigated [8], however most works do not consider such short duration fluctuations in the signal.

This work applies various machine learning (ML) methods to extract information from simulated hyperspectral time-series data, yielding information on the proportions of underlying materials and their evolution over time as the object rotates. This in turn is used to infer the presence of large components such as solar panels and antennas, and finally perform a classification of the targeted satellite. Applications of these techniques include reidentification of lost satellites, characterisation of unknown satellites, or characterisation of medium-large sized space debris.

2 Simulation Model

In order to produce sufficient quantities of training data for the ML models in later sections, physics and sensor simulations were developed to simulate hyperspectral sensor outputs. This simulation model takes as its input a low-polygon 3D model approximation of a given satellite (examples seen in Figure 1(a)) as

well as an initial orbit and rotation state vector. The trajectory and rotational kinematics are propagated according to the respective physical laws for some finite observation period.

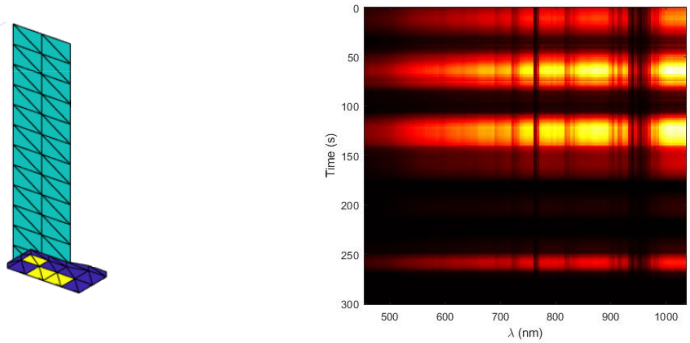

Fig. 1: (a) Example 3D representation of a Starlink satellite. Colours represent different 'regions' which are characterised by particular combinations of materials.
(b) Example simulated sensor output showing photon counts per band over time.

At each timestep, the light reflected from the object and collected by the receiver, in each sensor band, is calculated according to the Lambertian model of reflectance, accounting for time-varying occlusion and illumination conditions. Surface materials are modelled by using reflectance spectra $R(\lambda)$ corresponding to the underlying materials of each element in the 3D model. An example sensor output can be seen in Figure 1(b).

3 Data Processing Pipeline

The developed data processing pipeline is illustrated in Figure 2. The sensor data is first expressed in a format akin to colour indexing [5], which expresses intensity as relative to some reference band. This normalises for effects such as distance, which vary case-to-case, and enables learned relationships between band intensities to transfer to different physical configurations of the observer-satellite system.

The sensor data is then fed to an artificial neural network (ANN) which predicts the fraction of received light which is due to each present material at each time point. This model was trained on the ground truth output from the data generation simulation. The output of this model is a set of curves describing the abundance of each material over the observation arc. These are then converted into a set of 99 statistical features (mean, standard deviation, correlation coefficients, etc.) which are used as the inputs for the next model in the pipeline.

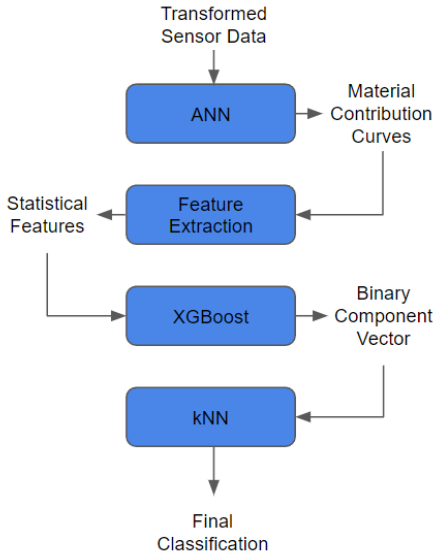

Fig. 2: Example simulated sensor output showing photon counts per band over time.

Following the ANN and feature extraction, a gradient boosted decision tree ensemble model (XGBoost) was used to predict the presence, or lack, of 5 large satellite components: solar arrays, antennas, thermal blankets, engine bells and optical baffles. Since all used 3D models were based on real satellites, a truth table could be constructed to use for training of this model.

Finally, the binary component vector output of the XGBoost model was passed to a k-Nearest Neighbours (kNN) algorithm to perform the final classification into the following classes:

- GNSS
- Earth Observation
- Communications
- Rocket Bodies
- CubeSats

Truth values for the final classification come from the nature of the underlying satellite - for example, DubaiSat is an Earth Observation satellite, Starlink is a comms satellite, etc.

4 Results and Generalisation

The material curve extraction model developed performs extremely well, and was able to recover the material abundances for objects composed of up to 9

materials (larger material libraries have not yet been tested). An example of these curves can be seen in Figure 3.

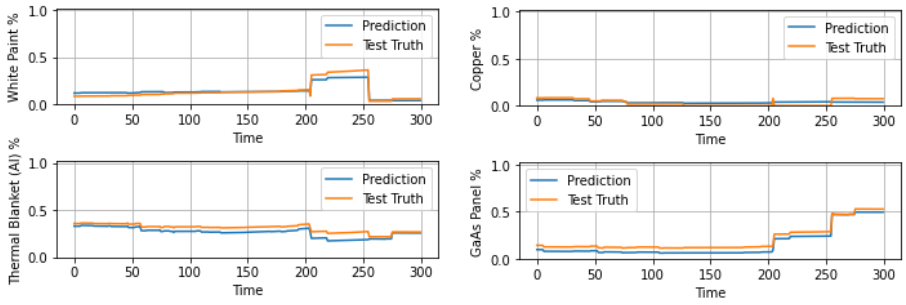

Fig. 3: Example of ANN material curve predictions compared with simulation ground truth.

The component detection model also performed very well, with low error rates as seen in Table 1.

Solar Panel	Engine Bell	Antenna	Optics	TPCB
1.0%	0.3%	2.6%	1.2%	2.0%

Table 1: Error rates for the component detection model.

To assess the performance of the component detection model on unseen satellites, the model was retrained multiple times, with each instance's training set having one satellite geometry excluded. The excluded class in each case was then used for testing. The error rates for each of these retrained models can be seen in Figure 4. It can be seen that the approach used for component detection generalises fairly well to unseen satellites, with the possible exception of optical baffles, which suffer a high error rate when certain satellites are excluded. This is perhaps due to the nature of the material being detected, black paint, which has a very flat reflectance curve of overall low magnitude, meaning there is little to detect insofar as spectral features.

When classifying with kNN based on the 5 listed compoents, the classes are not perfectly separable. However, there is only one case of overlap: Iridium-NEXT, a communications satellite, has a set of components which cause misclassification as GNSS even when components are correctly predicted. When training the XGB model on data from all satellites, this is the limiting factor in accuracy: with the exception of Iridium-NEXT, all satellites were correctly classified with over 99% accuracy.

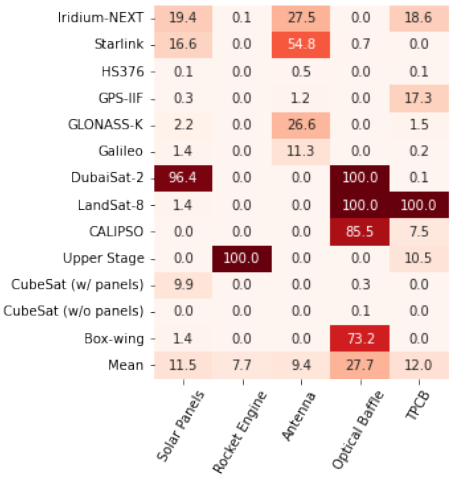

Fig. 4: Error rates for the 13 retrained XGB models, each time excluding and testing on one satellite type.

5 Summary

This work contributes a significant advancement in characterisation of space objects based on their reflectance spectra, and showed that significantly more detailed information may be extracted from time-varying spectral signatures than has previously been achieved. An ANN was used to extract the time-varying contribution of each underlying material on a rotating, orbiting object from ground. This information was then processed into a new set of features, before being fed to another ML model which predicts the presence of large, characteristic satellite components based on the underlying materials. This model was shown to be reasonably robust to satellites that were not included in the training set, however expanding the range of satellites in the training set would likely improve this model's generalisation further. Finally, an initial classification system based on kNN clustering of the component vectors was proposed. Although the classes were not perfectly separable, the separation was only violated by one specific satellite instance, and again, expanding the range of satellites used to produce training data may improve the kNN classification step.

Acknowledgements The authors would like to thank the European Space Agency for providing funding for this work, and to Emiliano Cordelli and Jan Siminski from ESA for their input and collaboration.

References

1. K. Jorgensen, J. Africano, K. Hamada, E. Stansbery, P. Sydney, P. Kervin: Physical properties of orbital debris from spectroscopic observations. Advances in Space

Research **34**(5), 1021-1025 (2004).
2. K. Abercromby, M. Guyote, J. Okada, et al.: Applying space weathering models to common spacecraft materials to predict spectral signatures. Proceedings of AMOS Technical Conference, 2005, Maui, Hawaii, USA.
3. J. A. Reyes, H. M. Cowardin, D. M. Cone: Characterization of space- craft materials using reflectance spectroscopy. Proceedings of the Advanced Maui Optical and Space Surveillance Technologies Conference, Maui, Hawaii, September 11-14, 2018.
4. T. Cardona, P. Seitzer, A. Rossi, F. Piergentili, F. Santoni: BVRI photometric observations and light-curve analysis of GEO objects. Advances in Space Research **58** (4) 514–527 (2016).
5. X.-F. Zhao, H.-Y. Zhang, Y. Yu, Y.-D. Mao: Multicolor photometry of geosynchronous satellites and application on feature recognition. Advances in Space Research **58** (11) 2269–2279 (2016).
6. A. Vananti, T. Schildknecht, H. Krag: Reflectance spectroscopy characterization of space debris. Advances in Space Research **59** (10) 2488–2500 (2017).
7. A. Willison, D. Bedard: A novel approach to modeling spacecraft spectral reflectance. Advances in Space Research **58** (7) 1318–1330 (2016).
8. E. Cordelli, P. Schlatter, T. Schildknecht: Simultaneous multi-filter photometric characterization of space debris at the Swiss Optical Ground Station and Geodynamics Observatory Zimmerwald. Advanced Maui Optical and Space Survaillance Technologies Conference (AMOS) (2018).